Bioconjugate Chemistry

Article

Cite This: *Bioconjugate Chem.* 2019, 30, 2469−2480

pubs.acs.org/bc

# Elucidating the Role of Surface Coating in the Promotion or Prevention of Protein Corona around Quantum Dots

Woody Perng, Goutam Palui,[†] Wentao Wang,[‡] and Hedi Mattoussi*

Department of Chemistry and Biochemistry, Florida State University, Tallahassee, Florida 32306, United States

Supporting Information

**ABSTRACT:** Nonspecific interactions in biological media can lead to the formation of a protein corona around nanocolloids, which tends to alter their behavior and limit their effectiveness when used as probes for imaging or sensing applications. Yet, understanding the corona buildup has been challenging. We hereby investigate these interactions using luminescent quantum dots (QDs) as a model nanocolloid system, where we carefully vary the nature of the hydrophilic block in the surface coating, while maintaining the same dihydrolipoic acid (DHLA) bidentate coordinating motif. We first use agarose gel electrophoresis to track changes in the mobility shift upon exposure of the QDs to protein-rich media. We find that QDs capped with DHLA (which presents a hydrophobic alkyl chain terminated with a carboxyl group) promote corona formation, in a concentration-dependent manner. However, when a polyethylene glycol block or a zwitterion group is appended onto DHLA, it yields a coating that prevents corona buildup. Our results clearly confirm that nonspecific interactions with protein-rich media are strongly dependent on the nature of the hydrophilic motif used. Additional gel experiments using SDS-PAGE have allowed further characterization of the corona protein, and showed that mainly a soft corona forms around the DHLA-capped QDs. These findings will be highly informative when designing nanocolloids that can find potential use in biological applications.

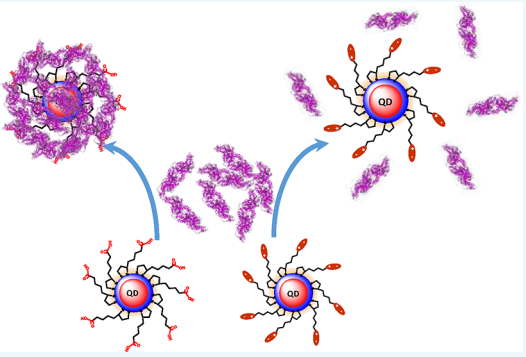




Inorganic nanocrystals with sizes typically in the range of 1−100 nm exhibit unique size- and composition-dependent optical and physical properties that are not observed for bulk materials or at the molecular scale.[1−5] For instance, colloidal core−shell nanocrystals made of semiconducting cores (often referred to as quantum dots), coated with an organic stabilizing shell, exhibit broad excitation spectra along with narrow and size-tunable emission profiles. This makes it possible to simultaneously excite different-sized QDs with a single monochromatic source and generate emissions at distinct wavelengths. In addition, luminescent QD materials have high quantum yields and exhibit remarkable resistance to chemical and photodegradation, along with enhanced two-photon action cross-section.[6−11] These unique properties have made them appealing for use in a wide range of potential applications in biology, including imaging, sensing, cell-targeting, and as delivery vehicles.[12−21]

A successful application that utilizes these nanomaterials in biology requires that the nanocrystals be compact in size and sterically stabilized over a broad range of conditions, and more importantly do not exhibit nonspecific interactions in biological media. It has been suggested that nanocrystals that are poorly stabilized or/and have highly charged surface coatings tend to promote nonspecific interactions with proteins and other biomolecules, when introduced into biological media; these media are naturally complex and contain a variety of proteins and ions. An absorbed layer of proteins on the nanocrystal surfaces is referred to as a "protein corona".[22−29] In most cases, protein coronas are detrimental to the integration of these materials within biological systems and for developing targeted applications. For instance, a protein corona may trigger aggregation of nanoparticles in biological media (e.g., cell cytoplasm, extracellular matrix, and blood), which in turn causes other problems, such as hampering the nanoparticle targeting efficiency or drastically reducing the blood retention time.[30] Over the past decade, numerous studies have investigated the origin of corona formation and attempted to characterize its structure and composition. Overall, research focusing on protein corona buildup on colloidal nanomaterials has centered on two broadly defined ideas. In the first, groups have tried to understand the correlation between the nature of the inorganic core, the surface coating strategy used, and the formation of adsorbed proteins. This includes efforts aimed at identifying the composition of the corona when present. In the second, efforts have focused on devising new surface-functionalization strategies that can promote long-term steric stabilization while drastically reducing or eliminating nonspecific interactions as a means of preventing corona buildup in protein-rich media. Studies have suggested that protein corona composition is affected by a few key factors, including the nature of the surface

**Received:** August 14, 2019
**Revised:** August 21, 2019
**Published:** August 26, 2019




DOI: 10.1021/acs.bioconjchem.9b00549
*Bioconjugate Chem.* 2019, 30, 2469−2480

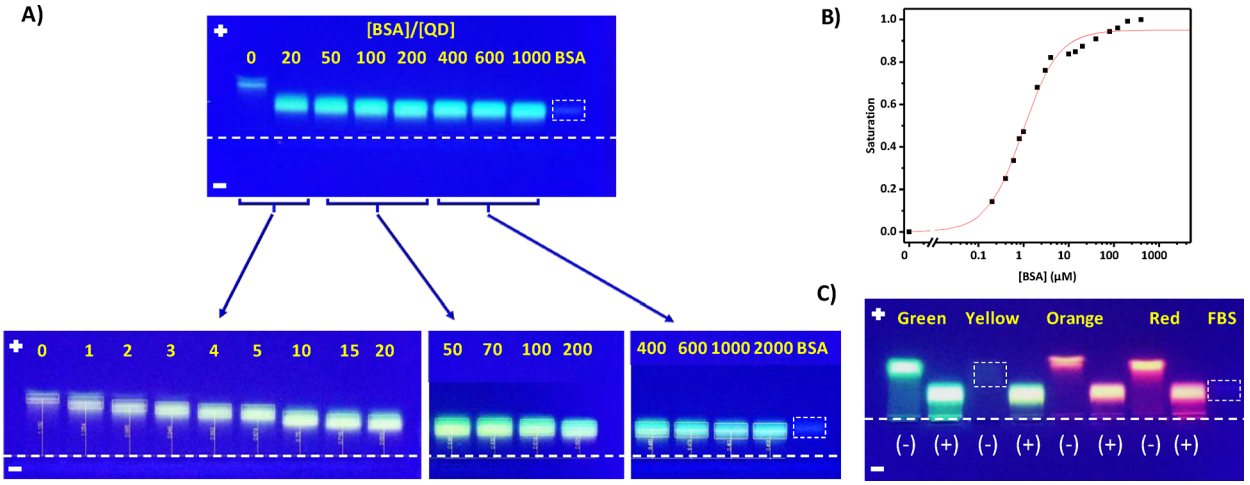


**Figure 1.** (A) Agarose gel electrophoresis images collected from DHLA-QDs after incubation with different molar ratios of BSA for 30 min at room temperature. The molar equivalent of [BSA] in the solution with respect to that of QDs is shown on top. The positive and negative signs (on the left) represent the anode and cathode, whereas the dashed line shows the position of the loading wells. (B) Plot of the saturation *S* vs [BSA] extracted from the gel data shown in panel A. The solid line is a fit to the Hill Equation. (C) Gel image collected from dispersions of QDs incubated with 10% FBS. The (−) and (+) signs indicate the absence and presence of FBS in the solution. The dashed rectangles outline the weak bands of yellow QDs and FBS. The bands associated with pure BSA and FBS are shown.

coating, the concentration of proteins, the incubation time, and the temperature.[31−42] Several reports have suggested that protein adsorption is highly dynamic, and in general, the surface adsorbed layer consists of a hard corona (composed of strongly bound proteins) and a soft corona (mainly made of weakly bound proteins).[23,32,43−45] Overall, prevention of corona buildup has mostly relied on manipulation and tuning of the surface chemistry of the colloidal nanomaterials. Two general surface coating schemes have been pursued. One relies on the introduction of various-sized poly(ethylene glycol) blocks in the surface coat.[46−48] The other exploits the dual ionic nature of zwitterion groups to reduce the overall dimension of the nanomaterials and to promote their dispersion in buffer media over a broad range of conditions, while reducing or eliminating protein adsorption.[49−51] Nonetheless, the structure and dynamic properties of the protein corona on nanocolloids remain complex and are still poorly understood.[52,53] Additionally, an in-depth understanding of the interactions of nanocolloids with biological systems is critically important for the safe integration of these materials in biological applications.

In the present study, we investigate the role of surface chemistry in preventing protein corona formation on luminescent QDs, surface ligated with a series of dihydrolipoic acid (DHLA)-based ligands, when mixed with bovine serum albumin (BSA), or with fetal bovine serum (FBS, a multiprotein-rich medium). Indeed, fetal bovine serum is a complex fluid that contains a large number of distinct proteins, with a total protein concentration of ∼450 $\mu$M.[54] This selection was motivated by (1) the similarities between fetal bovine serum and human serum, (2) the fact that 10% fetal bovine serum is routinely used in many cell culture experiments, and (3) the high abundance of albumin proteins in serum. We use agarose gel electrophoresis and SDS-PAGE (sodium dodecyl sulfate−polyacrylamide gel electrophoresis) to monitor corona formation and investigate its composition when possible. Factors such as surface chemistry, the use of PEG vs zwitterion, surface charge, and incubation time are tested.

## RESULTS AND DISCUSSION

**Rationale.** It has been known that even though the photophysical properties of nanocolloids, which are of interest to biology (e.g., absorption, emission, or magnetic signature), are strongly dependent on the composition and size of the inorganic cores, their stability in the solution phase is primarily controlled by the surface coating.[20,55,56] When dispersed in biological media, the coating is used to promote steric stabilization and reduce interactions with serum proteins. Consequently, controlled specific interactions, or nonspecific (less controlled) absorption onto the nanocolloids, are inherently dependent on the coating strategy employed to stabilize them.[57−60] Yet, despite several studies focusing on protein corona buildup on various nanomaterials, a direct and thorough investigation of the effects of tuning the nature of the coating (e.g., coordination vs encapsulation, presence or absence of charges) have not been sufficiently explored.

In this study, we use QDs that have been transferred to buffer media by ligand exchanging the native cap (TOP/TOPO, alkylamine, and alkylphosphine) with coordinating ligands based on the dihydrolipoic acid (DHLA) motif. DHLA-based ligands have been shown to exhibit higher affinity to ZnS-overcoated QDs and gold and silver nanocrystals than monothiol-appended ligands, for instance.[61−63] We tune the structure and size of the hydrophilic block, which plays a key role in promoting the dispersion of nanocrystals in physiological media.[61,64−66] Introducing functional groups such as amine, carboxylate, and methoxy groups gives rise to positive, negative, and neutral surface charges under physiological conditions. The use of PEG blocks or zwitterion moieties as hydrophilic motifs can change the overall hydrodynamic size of the nanocrystals and their affinity to water. The QD dispersions have been characterized using UV−vis absorption and photoluminescence spectroscopy before and after ligand exchange (see Supporting Information, Figure S1). The essentially identical features in both absorption and emission profiles indicate that cap exchange was successful and the core materials remained intact.



DOI: 10.1021/acs.bioconjchem.9b00549
*Bioconjugate Chem.* 2019, 30, 2469−2480

*Hydrophilic QDs with Dihydrolipoic Acid Capping.* We start with the simplest and smallest ligand motif of this family and perform cap exchange of the QDs with DHLA.[61,67] Dihydrolipoic acid is essentially made of a hydrophobic short alkyl chain with a terminal COOH. Because affinity to water relies on deprotonation of the carboxyl group, DHLA-capped QDs exhibit limited pH stability (with progressive aggregation forming at pH ≤ 6) and have relatively low quantum yield.[61] Furthermore, activation of the carboxyl groups (for the purpose of conjugation) produces progressive aggregation.[61,68] DHLA-QDs are, nonetheless, compact and have been successfully used to prove the assembly of QD−protein conjugates and design several energy transfer-based sensors.[69,70] These properties make DHLA-capped nanocrystals a good reference system to investigate corona formation on hydrophilic QDs. The QDs were mixed with BSA at molar ratios ranging from 1:0 to 1:2000, or with 10% FBS-supplemented PBS solutions for 30 min. Corona formation was monitored using agarose gel electrophoresis measurements, where changes in the mobility shift were tracked when the QDs were exposed to protein-rich solutions or media, compared to pure QD dispersions (serving as a reference). This test is simple yet informative, due to the sensitivity of the electrophoretic mobility to small changes in the surface charge or/and size of the overall QD-plus-adsorbed protein complexes. Additionally, the fluorescence properties of the QDs allow easy visualization of the materials in the gel, using excitation with a UV lamp.

Figure 1A shows representative agarose gel images collected from dispersions of DHLA-capped QDs mixed with varying concentrations of BSA. A protein control sample (BSA only) was included; the BSA band could be visualized by relying on its very weak autoflorescence signal. The gel image in panel A shows that the band for pure QDs is homogeneous and exhibits the largest mobility shift toward the anode (+), a property attributed to the presence of a large number of chargeable carboxylic groups around the nanocrystal (one per surface ligand). The figure also shows that as the concentration of BSA increases, the mobility shift gradually decreases, indicating that the overall size and surface charge of the fluorescent nanocrystals in the sample have been altered in a concentration-dependent manner. Interestingly, the most pronounced change in mobility shift takes place for [QD]:[BSA] molar ratios ranging from 1:0 to 1:20, followed by progressive saturation reached at higher protein concentrations (at QD:BSA exceeding 1:50; see Figure 1A).

We attribute this behavior to nonspecific (mostly charge or electrostatically driven) adsorption of BSA proteins onto the nanocrystals, i.e., formation of a protein corona around the QD surfaces. Changes in the degree of BSA adsorption are more pronounced at smaller protein concentrations, but slowly saturate as the molar excess of proteins becomes larger. Assuming that the mobility of the nanocrystals in the gel is directly affected by the amount of surface-absorbed BSA, one can then use a plot of the changes in the mobility shift as a function of the QD:BSA molar ratio, to extract a saturation plot for the data and gain insights into the BSA binding affinity onto the QD surfaces (shown in Figure 1B). The saturation curve is generated from the data on the mobility shift using

$$S = \frac{d_0 - d}{d_0 - d_{sat}} \quad (1)$$

where $d_0$, $d$, and $d_{sat}$, respectively, designate the migration distance (from the loading well) corresponding to [BSA] = 0, at any given value of [BSA], and at saturation concentration. The data can be fit to a sigmoidal curve using the Hill equation expressed as[71]

$$y = a \times \frac{[BSA]^n}{K_d + [BSA]^n} \quad (2)$$

Fitting the saturation vs [BSA] curve to eq 2 yields a value for the apparent dissociation constant ($K_d$), corresponding to 50% saturation, while the Hill constant ($n$) is usually used to infer information about cooperativity in the interactions (here between proteins and QDs).[71,72] The experimental curve shows a well-defined, S-shaped profile routinely observed for systems with strong interactions.[72] The best fit to the experimental data was achieved using $n$ = 1.1 ± 0.1 (i.e., ∼1) and $K_d$ ∼ 0.96 μM, which implies that protein adsorption buildup on DHLA-capped QDs is essentially noncooperative. In other words, the binding of new proteins is independent of those already adsorbed on the NP surfaces. (**Remark:** We would like to note that in eq 1 we used the more commonly employed definition for the dissociation constant, $K_d = k_{off}/k_{on}$, where $k_{on}$ and $k_{off}$ are the intrinsic association (binding) and dissociation rates, respectively. In our previous reports, we used the opposite definition for the dissociation constant: $K_d^{-1} = k_{off}/k_{on}$.[73,74])

We expanded this test to probe the effects of mixing a few sets of DHLA-capped QDs (having different core sizes, with green, yellow, and red emissions) with a relatively more complex system that mimics physiological conditions using 10% fetal bovine serum (in PBS). Dispersions of QDs alone and QDs mixed with FBS were loaded into adjacent wells to allow a side-by-side visual comparison of changes in the electrophoretic mobility upon exposure to the media (see Figure 1, panel C). Pure QD dispersions and a solution of 10% FBS were included as references. The gel image in Figure 1C shows that a pronounced reduction in the mobility shift is measured for all four sets of QDs when incubated with FBS. In addition, the positions of retarded bands are similar to those measured for QDs mixed with BSA at the largest molar excess shown in Figure 1A. Our findings agree with the results reported by Nienhaus, Parak, and co-workers who used fluorescence correlation spectroscopy (FCS) to probe the corona buildup of human serum albumin (HSA), succinic anhydride-modified HSA (HSAsuc), and ethylenediamine-modified HSA (HSAam) around DHLA-QDs, by tracking changes in the hydrodynamic radius of the nanocrystals with increasing protein concentration.[75,76] Furthermore, they measured the differences in the degree of adsorption between those three closely related proteins.

We should also note that there is an enhancement in the fluorescent band intensity upon mixing with proteins or FBS. Such an enhancement is commensurate with the protein concentration, with saturation occurring at [BSA] ∼ 4 μM (approximately at a molar equivalent of 20 BSA per QD). This result is similar to what we previously reported for DHLA-QDs self-assembled with polyhistidine-appended proteins,[67,77] and provides further proof (though indirect) that protein adsorption onto DHLA-QDs is the cause for the changes in the measured electrophoretic mobility.

*QDs Capped with PEG- or Zwitterion-Modified DHLA.* The next set of measurements tested the effects of attaching a


DOI: 10.1021/acs.bioconjchem.9b00549
Bioconjugate Chem. 2019, 30, 2469−2480

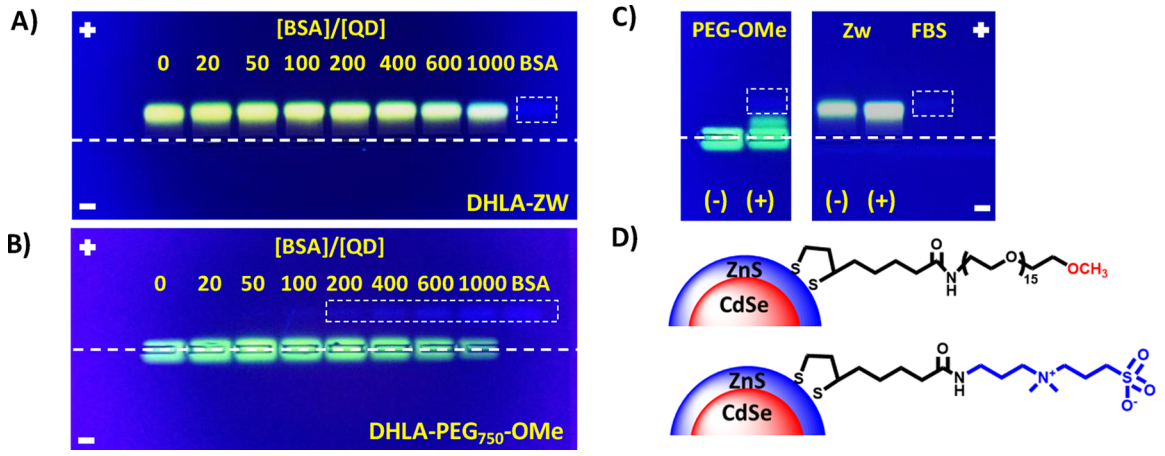


**Figure 2.** Agarose gel images collected from (A) DHLA-ZW-QDs and (B) DHLA-PEG$_{750}$-OMe-QDs incubated with increasing molar amounts of BSA. (C) Gel images of DHLA-PEG$_{750}$-OMe-QDs and DHLA-ZW-QDs before (−) and after (+) incubation with 10% FBS. The QDs were incubated with the proteins at room temperature for 30 min. The dashed rectangles designate the bands associated with the mobility bands of BSA or FBS alone in the various configurations. (D) Schematic representation of the two coatings used, namely, DHLA-PEG$_{750}$-OMe and DHLA-ZW.

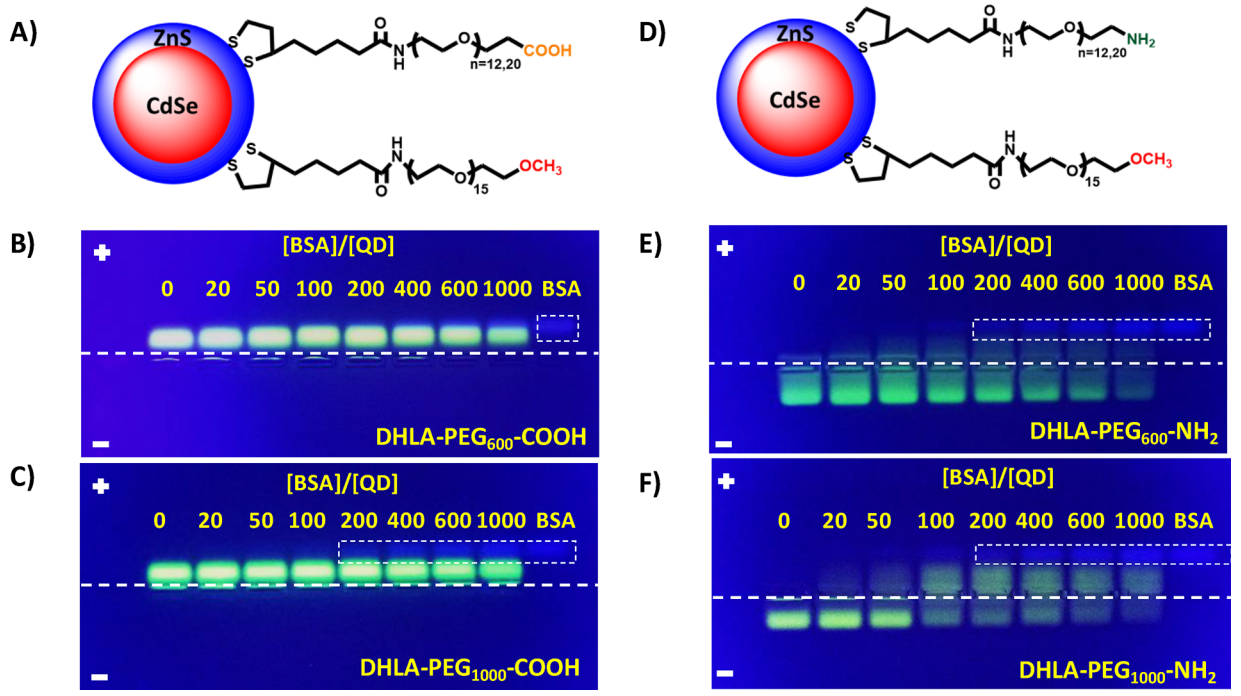


**Figure 3.** Schematic representations of the two sets of hydrophilic QDs are shown: (A) DHLA-PEG-COOH-QDs and (D) DHLA-PEG-NH$_2$-QDs. Agarose gel images acquired from QDs capped with different combinations of ligands and incubated with increasing molar excess of BSA: (B) DHLA-PEG$_{600}$-COOH-QDs; (C) DHLA-PEG$_{1000}$-COOH-QDs; (E) DHLA-PEG$_{600}$-NH$_2$-QDs; (F) DHLA-PEG$_{1000}$-NH$_2$-QDs.

hydrophilic motif made of either a polyethylene glycol block or a zwitterion (*N*,*N*-dimethylpropanediamine-sulfobetaine) group at the lateral end of DHLA, as a means of potentially controlling the nonspecific interactions with proteins. Indeed, the use of PEGylated coating has been discussed by a few groups as effective for reducing the corona buildup on AuNPs, though larger PEG blocks (~5 kDa) have often been employed.[42,47] While PEG-OMe is overall neutral, both cations and anions are simultaneously present in a zwitterion group. As such, two agarose gels have been loaded with dispersions of QDs ligated with DHLA-PEG$_{750}$-OMe or DHLA-ZW preincubated with BSA at QD:BSA molar ratios ranging from 1:0 to 1:1000. Figure 2A,B shows representative images collected from gels loaded with dispersions of DHLA-ZW-QDs and DHLA-PEG-OMe-QDs, respectively. Clearly, no change in the mobility shift is observed for any [BSA] value (compared to the QDs alone) for either set of QDs. Additionally, while an essentially zero mobility shift has been measured for DHLA-PEG$_{750}$-OMe-capped QDs, a constant positive mobility shift toward the anode has been measured for DHLA-ZW-capped QDs (compare gels in Figure 2A and B). This difference can be traced back to the fact that PEG-OMe blocks are overall neutral across a wide pH range, while the sulfobetaine groups endow the nanocrystal surfaces with a net negative charge across a wide pH range, which promotes a positive mobility shift (toward the anode, see Figure 2A).[78] This net negative charge (or zeta potential) originates from the differential binding of counterions in the surrounding solution



DOI: 10.1021/acs.bioconjchem.9b00549
*Bioconjugate Chem.* 2019, 30, 2469−2480

onto the positive and negative groups of the zwitterion, following the hard/soft acid/base principle.[79] We also probed the effects of mixing the QDs with 10% FBS (in PBS) on the mobility of the two sets of DHLA-ZW- and DHLA-PEG-OMe-stabilized QDs. The image shown in Figure 2C indicates that no change in the mobility shift is measured for DHLA-ZW-QDs, though a slight tailing of the band can be seen in the well loaded with DHLA-$PEG_{750}$-OMe-QDs. The slight tailing observed for the PEG-OMe-QDs-plus-10% FBS mixture (Figure 2C) can be attributed to the presence of weak, heterogeneous interactions with minor proteins in FBS. These observations combined indicate that there are essentially no measurable changes in the overall dimensions, or charge of the QDs upon mixing with the proteins at any concentration. We can thus infer that introduction of a short PEG-OMe block or a ZW group in the coating eliminates nonspecific adsorption of BSA and other proteins in the FBS media for these QDs. These findings are in agreement with the results reported by Parak and co-workers.[80] They also showed that the DHLA-ZW coating drastically reduces protein adsorption on luminescent QDs using FCS measurements. The ability of zwitterion groups to provide strong steric stabilization for the QDs and to eliminate the nonspecific absorption of proteins, despite their very small size compared to PEG blocks, can be attributed to the rather strong electrostatic interactions with water molecules, leaving the hydrogen bonding structure with water molecules unperturbed (compared to bulk water). This in turn renders it difficult to replace the layer of water molecules around the zwitterion-coated nanocrystals with proteins or other biomolecules.[81]

It has been suggested that the ability of the PEG coating to promote long-term steric stability and reduce nonspecific interactions may be dependent on the presence of terminal functional groups in the ligands.[82] Additionally, using higher molecular weight PEG blocks (e.g., MW ∼ 5 kDa) can reduce the affinity to water combined with a decrease in the ligand density on the NP surfaces (due to the size increase in the polymer coil size).[45,48,83] We investigated this issue by introducing terminal carboxyl or amine groups at the lateral end of the PEG coating using two sizes of PEG moieties, $PEG_{600}$ and $PEG_{1000}$; additional details on the synthesis of these compounds is provided in refs 68 and 84. More precisely, we used four sets of QDs, (1) one coated with a mixture of DHLA-$PEG_{750}$-OMe and DHLA-$PEG_{600}$-COOH (referred to as QD-$PEG_{600}$-COOH); (2) one coated with a mixture of DHLA-$PEG_{750}$-OMe and DHLA-$PEG_{1000}$-COOH (referred to as QD-$PEG_{1000}$-COOH); (3) one coated with a mixture of DHLA-$PEG_{750}$-OMe and DHLA-$PEG_{600}$-amine (QD-$PEG_{600}$-$NH_2$); and (4) one coated with a mixture of DHLA-$PEG_{750}$-OMe and DHLA-$PEG_{1000}$-amine (QD-$PEG_{1000}$-$NH_2$); the same OMe:COOH/$NH_2$ molar ratio of 70:30 has been used for all four sets of QDs. These provide a broad set of conditions to explore. The dispersions were mixed with increasing concentrations of BSA before loading onto agarose gels. The gel images in Figure 3B,C show that a finite mobility shift toward the anode has been measured for both sets of PEG-COOH-QDs, regardless of the molar concentration of added BSA. We should note that the mobility bands of free BSA are slightly more resolved from those of the QD bands for DHLA-$PEG_{1000}$-COOH-capped nanocrystals compared to what is observed for nanocrystals presenting DHLA-$PEG_{600}$-COOH capping, a result that can be attributed to the slightly larger overall size of $PEG_{1000}$-coating (i.e., larger PEG block). The migration of $PEG_{1000}$-QDs in the gel is thus smaller than that of $PEG_{600}$-QDs, yielding mobility bands for $PEG_{1000}$-coated QDs that are more resolved from those of BSA. The absence of any change in the mobility shift with BSA is overall similar to the one observed for PEG-OMe-QDs. However, a negative mobility (shift toward the cathode) is measured for both sets of QD-PEG-$NH_2$ (i.e., in the absence of proteins), combined with progressive reduction and smearing of the bands as the BSA concentration is increased. The gel image shows that band smearing at higher [BSA] extended to positive mobility. The change in the mobility shift (band position) and, more importantly, the smearing measured at higher [BSA] indicate that the terminal amine groups on the QD surfaces promote some degree of nonspecific interactions and protein adsorption. Nonetheless, those interactions are rather weak and generate heterogeneous distributions of adsorbed proteins on the nanocrystals, which manifests in the substantial smearing of the mobility bands to include "negative" and "positive" shifts, as seen in Figure 3E,F.

These experiments were supplemented with gel electrophoresis measurements using the above QD dispersions (presenting COOH and amine groups) mixed with 10% FBS solutions. Gels loaded with the green- and red-emitting QDs having the same combinations of carboxyl and amine coatings are shown in Figure 4A and B, respectively. Overall, the data

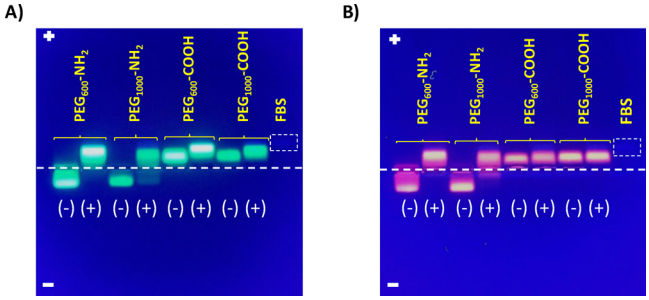


**Figure 4.** Agarose gel images of green- (A) and red-emitting (B) QDs with the various combinations of capping ligands, incubated with 10% FBS. The anode and cathode are indicated in white, while the dashed line shows the position of the loading wells. The (+) and (−) signs indicate with and without incubation with FBS solution, respectively. The mobility bands for pure FBS are also shown (dashed white rectangles).

support the main observations recorded for QD dispersions mixed with BSA above. In the presence of FBS, the QD-PEG-$NH_2$ samples exhibit negative mobility shifts with net migration toward the cathode. There is smearing in the mobility bands for both conditions (with and without FBS). We should also note that the band smearing is less pronounced in the presence of FBS, as these media have rather large concentration of proteins. However, the mobility shift measured for QD-PEG-COOH is marginally changed after mixing with FBS, an observation that is consistent with the data shown in Figure 3 above. We should add that similar results were obtained from yellow- and orange-emitting QDs (see Supporting Information, Figure S2). Overall, the effects of changing the PEG segment molecular weight from 600 to 1000 are negligible. This implies that nonspecific interactions with BSA, or with a wider range of proteins present in FBS, are more dependent on the nature of the chargeable functionalities in the PEG coating, with amine groups yielding nanocrystals that are more susceptible to nonspecific protein adsorption


DOI: 10.1021/acs.bioconjchem.9b00549
Bioconjugate Chem. 2019, 30, 2469−2480

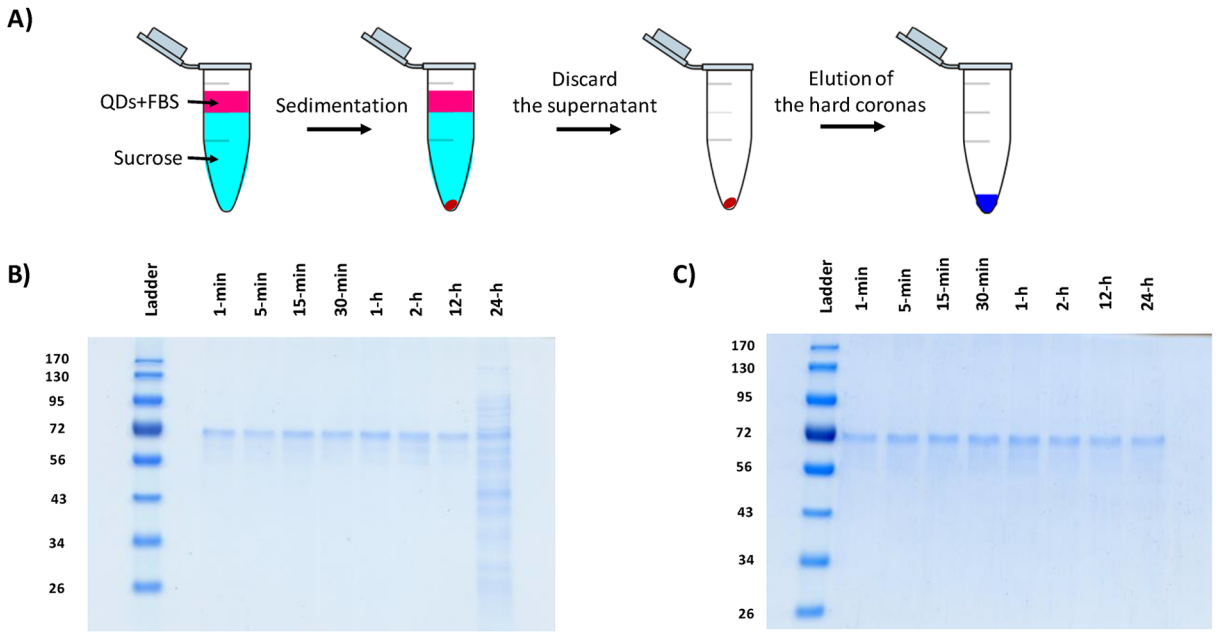


**Figure 5.** (A) Schematic representation of the sucrose cushion along with centrifugation and elution steps, applied during the SDS-PAGE experiments. (B,C) SDS-PAGE image collected from dispersions of DHLA-QDs and DHLA-$PEG_{750}$-OMe-QDs, respectively. Samples were incubated with 10% FBS at room temperature for 1 min, 5 min, 15 min, 30 min, 1 h, 2 h, 12 h, and 24 h.

than carboxyl groups. However, shorter PEG-COOH coatings ($PEG_{400}$ and smaller) have been reported to exhibit a stronger tendency to promote nonspecific interactions in protein-rich media.[82]

*Semiquantitative Densitometry Analysis.* The buildup of a protein corona around colloidal nanomaterials has been divided into two types, as proposed by Dawnson's group and others:[32,85] (1) Soft corona is formed when reversible adsorption of proteins onto the nanocrystals takes place, yielding a weakly bound layer that can be detached by a combination of buffer washing and centrifugation. (2) Hard corona refers to a strongly adsorbed layer of proteins. Here, removal of the proteins cannot be simply achieved by washing and centrifugation, as done above, but rather incubation with a detergent-containing buffer (such as $\beta$-mercaptoethanol, BME, or sodium dodecyl sulfate, SDS) is needed. Indeed, agarose gel electrophoresis measurements alone cannot distinguish between the two types of coronas, since under the conditions used the nanocrystal-plus-protein layer (weakly or strongly bound) migrates throughout the gel pores as a unit. Thus, agarose gel electrophoresis measurements were complemented with SDS-PAGE experiments and semiquantitative densitometry analysis, to identify whether or not the protein layer formation produces soft or hard, or a combination of both types of coronas. In addition, protein adsorption onto nanocolloids requires sufficient incubation time to ultimately promote corona buildup. Thus, investigating the effects of protein concentration and incubation time would yield additional insights into how nonspecific interactions do or do not promote protein layer assembly around a nanocrystal.

We have incubated dispersions of DHLA-QDs and DHLA-$PEG_{750}$-OMe-QDs with 10%FBS, for time periods of 1 min, 5 min, 15 min, 30 min, 1 h, 2 h, 12 h, and 24 h. The excess unbound or weakly adsorbed proteins were then separated from the QD-bound ones by applying three rounds of sucrose cushion centrifugation followed by one round of washing using PBS buffer (see schematics in Figure 5A). Additional experimental details on the procedure can be found in the Experimental Section. Figure 5B shows a representative SDS-PAGE image collected from dispersions of DHLA-capped QDs incubated with the media for varying times. The gel shows the presence of a weak intensity protein band at 70 kDa for incubation times from 1 min to 12 h. However, for 24 h incubation multiple weak intensity bands spreading from higher to lower molecular weights are observed. In comparison, the SDS-PAGE image collected from dispersions of DHLA-$PEG_{750}$-OMe-capped QDs show that only one weak intensity band at 70 kDa is measured, independent of the incubation time up to 24 h (see Figure 5C).

These data indicate that the amount and the composition (i.e., band profile) of recovered proteins is essentially unperturbed for dispersions of DHLA-$PEG_{750}$-OMe-capped QDs. In comparison, for DHLA-capped QDs the makeup of the recovered protein mixture formed during incubation changed with time, consistent with the Vroman effect.[86]

An additional experiment using SDS-PAGE has been performed to investigate changes in the composition of strongly bound proteins on the same set of QDs when incubated with 5%, 10%, 20%, 40%, 60%, 80%, and 98% FBS in PBS solution for 30 min, which mimics protein concentrations often encountered in vitro (smaller % FBS) and in vivo (larger % FBS) conditions. The gel data collected under those conditions show the presence of a weak intensity band at 70 kDa, regardless of the protein concentration in the FBS media for either set of QDs (see Supporting Information, Figure S3). This implies that under the incubation conditions used, the amount of bound protein is very small. In addition, there is no measurable effect of incubation concentration on the composition of those proteins. Identification of the most abundant proteins present in the corona formed on red-emitting DHLA-capped QDs was carried out using UPLC-MS/MS measurements (see Supporting Information). We find


DOI: 10.1021/acs.bioconjchem.9b00549
*Bioconjugate Chem.* 2019, 30, 2469−2480

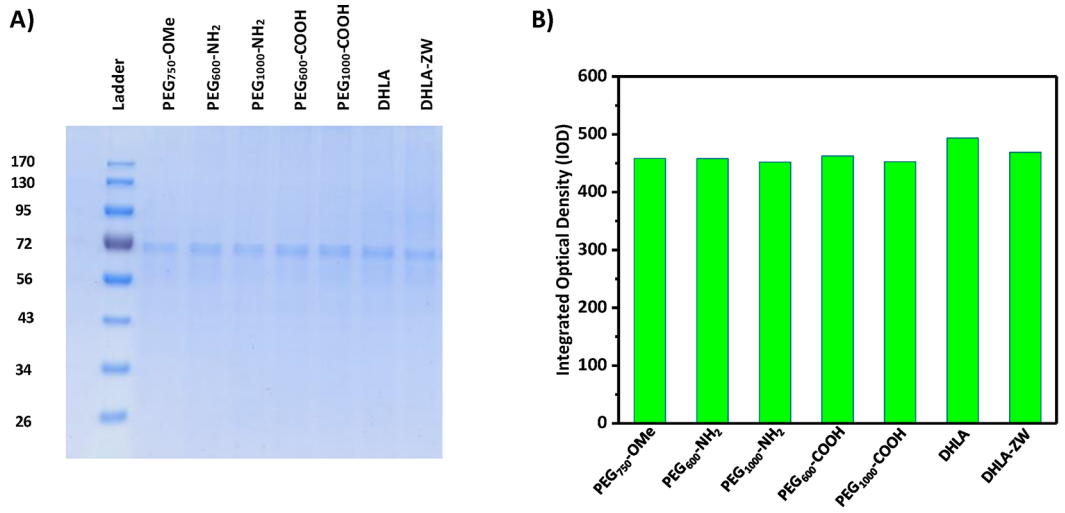


**Figure 6.** (A) SDS−polyacrylamide gel electrophoresis image from QDs (green emitting) capped with different combinations of DHLA-based ligands. (B) Integrated optical density of the bands shown in the gel. The peaks were integrated over the molecular weight ranges of ∼56−72 kDa and ∼80−95 kDa. Data collected from dispersions of red-emitting QDs are shown in the Supporting Information, Figure S5.

that over the range spanning 95−56 kDa, the dominant proteins are essentially $\alpha$-2-HS-glycoprotein and serum albumin (see Supporting Information, Table S2).

We further characterized the amount of proteins in the "hard corona", by performing semiquantitative densitometry analysis of the bands in the SDS-PAGE images. Figure 6 panel A shows a representative SDS-PAGE image collected from QDs, surface-capped with the various DHLA-based ligands (DHLA-PEG$_{750}$-OMe, DHLA-PEG$_{600/1000}$-NH$_2$, DHLA-PEG$_{600/1000}$-COOH, DHLA, and DHLA-ZW) incubated with 10% FBS for 30 min. A set of BSA solutions with known concentrations were included in the gel, as standards for quantification purposes (see Supporting Information, Figure S4). The data show that for all QDs, only a weak band at 70 kDa is measured for these dispersions. Quantification of the amounts of detected proteins was extracted from the integrated band intensities using Gel-Pro Analyzer and summarized in Table 1. Overall, the data show that regardless of the exact structure of the coating used, the estimated molar amounts of "hard corona" per QD is rather small, ∼0.67−0.72 (i.e., less than one protein per QD). Similar results were obtained using red-emitting QDs (see Supporting Information, Figures S5 and Table S2).

**Table 1. Quantification of Strongly Bound Proteins ("Hard Corona") on Green-Emitting QDs, Surface-Capped with Different Ligand Structures**[a]

| ligand coating | IOD | pmol of proteins | pmol of QDs | protein/QD |
|---|---|---|---|---|
| DHLA-PEG$_{750}$-OMe | 458.32 | ∼75 | ∼100 | ∼0.67 |
| DHLA-PEG$_{600}$-NH$_2$ | 458.03 | ∼75 | ∼100 | ∼0.66 |
| DHLA-PEG$_{1000}$-NH$_2$ | 452.01 | ∼72 | ∼100 | ∼0.63 |
| DHLA-PEG$_{600}$-COOH | 462.66 | ∼78 | ∼100 | ∼0.69 |
| DHLA-PEG$_{1000}$-COOH | 452.62 | ∼72 | ∼100 | ∼0.63 |
| DHLA | 493.53 | ∼96 | ∼100 | ∼0.85 |
| DHLA-ZW | 469.06 | ∼82 | ∼100 | ∼0.72 |

[a]The integrated optical density (IOD) was measured for each band using Gel-Pro Analyzer.

We now discuss our findings within the framework of soft corona formation around the surfaces of DHLA-capped QDs, promoted by nonspecific, electrostatically driven interactions with proteins in biological media. Our data show that protein adsorption around the QDs is measured for the coating that provides the weakest steric stabilization of the QDs in hydrophilic media.[75] The amount of adsorbed proteins depends on the BSA concentration, with a pronounced buildup occurring at low concentrations before slowly reaching saturation at larger values (see Figure 2). Protein adsorption on the QDs is noncooperative, with a dissociation constant of ∼1 $\mu$M. When a short PEG block (∼600−1000 Da) or a zwitterion group is introduced at the lateral end of the DHLA anchor, the amount of absorbed protein measured per QD is essentially negligible.[80] The SDS-PAGE data and the densitometry analysis imply that the adsorbed proteins primarily form a soft corona around the nanocrystals. The formation of a soft corona around DHLA-capped QDs, combined with the absence of any protein adsorption onto PEGylated or zwitterion DHLA coating, can be attributed to the stronger affinity of DHLA anchors compared to their monothiol counterparts. The high affinity of DHLA to the QD surfaces would prevent competitive desorption of the ligands, a property not guaranteed when monothiol-PEG or other weak coatings are used. Ligand desorption would allow direct protein interactions with the inorganic surfaces and ultimately corona buildup.

The presence of terminal amine groups in the DHLA-PEG coating can promote reversible nonspecific protein adsorption (soft corona), while carboxyl groups do not. This result is consistent with prior findings indicating that amine-QDs (with or without PEG blocks) tend to exhibit nonspecific interactions with cell cultures.[87] It implies that electrostatic attractions between the amine-QDs and negatively charged proteins in media or with membranes in cell cultures dominate the interactions. Overall, our results imply that a combination of strong coordination and a judicious choice of the hydrophilic motif (e.g., a zwitterion group or a PEG block with MW ∼600−1000 Da) is more effective for potentially eliminating the protein corona buildup around QDs and other nanocolloid surfaces.



DOI: 10.1021/acs.bioconjchem.9b00549
Bioconjugate Chem. 2019, 30, 2469−2480

We would like to stress that our conclusion stating that the adsorbed protein layers formed around the DHLA-capped QDs are primarily made of soft corona differs from the one reported by Nienhaus and co-workers in ref 76. Their analysis of the corona did not include multiple incubations with a sucrose cushion followed by centrifugation. Our approach used the protocol detailed by Stauber and co-workers,[28,88] which established that an unequivocal identification of the corona type requires multiple incubations with a sucrose cushion, each followed by one round of centrifugation. We found that when one round sucrose cushion centrifugation was applied, the SDS-PAGE image of the supernatant showed the presence of a strong protein band spanning a broad molecular weight range, including 56 and 70 kDa (see Supporting Information, Figure S6).

## CONCLUSION

We have probed the nonspecific interactions of serum proteins with luminescent QDs and the potential corona formation under varying surface coating formulations. For this, we used core−shell QDs, surface coated with a set of ligands with varying structures and hydrophilic blocks, based on the DHLA coordinating motif. Factors such as the structure of the water-solubilizing block (zwitterion vs PEG), the length of the PEG block, and the presence or absence of terminally chargeable groups have been probed. We found that in the absence of a clearly defined hydrophilic block (i.e., affinity to water is promoted by the presence of carboxyl groups), protein adsorption leading to corona formation around the nanocrystals took place. In comparison, introducing a PEG block (with MW = 600−1000 Da) or a sulfobetaine zwitterion group into the ligand essentially prevented protein adsorption on the nanocrystals. We also found that when a fraction of the coating ligands (in a mixed surface ligands coating) presented amine groups, non-negligible adsorption of BSA formed without clearly producing features associated with a corona layer, but ultimately a better-defined corona formed in a more complex fluid (i.e., FBS). Combining agarose gel with SDS-PAGE measurements allowed us to show that the adsorbed layer for DHLA-capped QDs is primarily made of soft corona. These results show that the nature and structure of the organic coating plays a major role in promoting or preventing protein adsorption on nanocolloids. Additional tests using other colloidal nanocrystals with different shapes and core material compositions, or/and polymer-based coordinating ligands based on the DHLA or other motifs (such as imidazole and phosphonate) for surface functionalization, can provide additional information on the behavior of a broad range of nanomaterials in biological media. We anticipate that information extracted from such studies will help in designing highly stabilized nanocolloids that prevent nonspecific interactions with great potential for use in biological studies.

## EXPERIMENTAL SECTION

**Quantum Dot Growth.** In this study, different sets of CdSe-ZnS core−shell QDs with emission wavelength varying from 537 nm (green) to 606 nm (red) were prepared following previous protocols.[8,9] The QD dispersions were prepared via reduction of the organometallic precursors in a hot coordinating solvent mixture made of surfactant and coordinating molecules, in a two-step reaction. In the first step, core CdSe nanocrystals were grown first via the reduction of cadmium and selenium precursors at ∼300−350 °C using a solvent mixture made of trioctyl phosphine (TOP), trioctyl phosphine oxide (TOPO), and hexamethylenediamine (HDA), along with a small fraction (4−5% in w/w) of hexylphosphonic acid (HPA); these solvent molecules are also known to coordinate onto the QD surfaces.[63] The core nanocrystal size was controlled by varying the concentration of the precursors used and by adjusting the annealing temperature. The CdSe cores were then overcoated with a few monolayers (here ∼5−6 monolayers) of ZnS using zinc and sulfur precursors at lower temperature (150−180 °C). More details can be found in ref 63.

**Ligand Synthesis.** The polyethylene glycol-appended lipoic acid ligands used in this study, namely, LA-PEG$_{750}$-OCH$_3$, LA-PEG-NH$_2$, and LA-PEG-COOH, were prepared, purified, and characterized following the procedures we described in our previous reports.[84,89] The LA-appended with zwitterion (LA-*N*,*N*-dimethylpropanediamine-sulfobetaine) ligands was synthesized following the steps detailed in ref 91. Chemical reduction of the dithiolane groups to provide the dihydrolipoic acid (DHLA)-modified compounds used for the ligand exchange of the hydrophobic QDs and phase transfer was carried out using sodium borohydride, as described in ref 84. Synthesis of other ligands is provided in the Supporting Information.

**Ligand Exchange.** Ligand exchange and phase transfer were carried out in three steps: (1) precipitation of the hydrophobic nanocrystals to discard excess free native ligands; (2) mass action driven substitution of the hydrophobic coating with DHLA-PEG ligands; and (3) purification of the nanocrystals by removing the solubilized hydrophobic coating molecules and excess free hydrophilic ligands. Briefly, a stock dispersion of hydrophobic CdSe-ZnS QDs (∼8 μM, 200 μL) was precipitated using excess ethanol, and the procedure was repeated once.[89] Then, ∼40 mg of DHLA-PEG ligands dissolved in methanol (400 μL) was mixed with the QD-pellet and further sonicated until the QDs were completely redispersed in the solution. The mixture was stirred at 60 °C overnight, and the QDs were precipitated by adding 200 μL of methanol and excess hexane. After sonication, the monophasic−turbid solution was centrifuged for 5 min at 3700 rpm, yielding an orange pellet. The clear supernatant was discarded, and the pellet was redispersed in a 50:50 mixture of chloroform and methanol (400 μL total), followed by precipitation using excess hexane. After centrifugation, the residual precipitate was dried under vacuum for 15 min. The pellet was dispersed in DI water, then passed through a 0.45 μm syringe filter. In addition, excess free ligands were removed by applying 3 rounds of concentration/dilution with DI water using a centrifugal filtration device (Millipore, Mw cutoff = 50 kDa).

The above procedure can also be applied to DHLA (no PEG block) with few modifications. Following precipitation of the hydrophobic QDs with excess ethanol, the resulting pellet was mixed with the pure ligand (∼100 μL) and sonicated until the dispersion became homogeneous. The mixture was stirred at 70 °C overnight, followed by the addition of DMF (1 mL). The QDs were then precipitated by adding potassium *tert*-butoxide.[63] After sonication, the monophasic, turbid solution was centrifuged for 5 min at 3700 rpm. The clear supernatant was discarded, and the pellet was dried and redispersed in water. The pH of the solution was adjusted to pH 10 by the addition of potassium *tert*-butoxide, which yielded a clear homogeneous dispersion in water.


DOI: 10.1021/acs.bioconjchem.9b00549
*Bioconjugate Chem.* 2019, 30, 2469−2480

Cap exchange with LA-ZW did not use the chemically reduced form. Instead, LA-ZW was photochemically ligated onto the QD in situ using a UV signal.[90,91] Briefly, a dispersion of QDs in hexane was mixed with an equal volume of LA-ZW solution in methanol (in a scintillation vial), yielding a two-phase solution made of TOP/TOPO-capped QDs in hexane (top) and LA-ZW in methanol (bottom). A stir bar was introduced and the vial was placed in a UV reactor (Luzchem UV lamp, model LZC-4 V) and irradiated for ∼40 min while stirring. This produced a nanocrystal precipitate, due to the poor solubility of the ligated QDs in methanol. The clear supernatant was discarded and the pellet was further washed with methanol (∼500 μL) twice followed by centrifugation for 5 min at 3700 rpm. The QD-pellet was dried under vacuum and then redispersed in DI water, yielding a clear and homogeneous dispersion.

**Gel Electrophoresis.** *Agarose Gel Electrophoresis.* The gel electrophoresis measurements applied to dispersions of the QDs alone and QDs mixed with BSA were carried out using a 0.5% agarose gel and tris borate EDTA buffer (TBE, 89 mM tris, 89 mM boric acid, 1 mM EDTA). The stock dispersion of nanocrystals was mixed (in Eppendorf tubes) with BSA solutions at different molar ratios, and then diluted to the desired final volume by adding phosphate saline buffer (pH 7.4, 20 mM). The final QD concentration was 0.2 μM, while the molar ratio of BSA with respect to QDs was varied from 0 to 1000. The concentration of FBS was fixed at 10% (v/v). The content of each sample was incubated for 30 min at room temperature, and then mixed with 2.5 μL of loading buffer made of Ficoll 400, immediately prior to use. 25 μL aliquots of these mixtures were loaded into the gel wells, and then a voltage of 6.0 V/cm was applied for 40 min to promote the electrophoretic migration of the QDs. The bands were imaged under fluorescence mode (using a UV excitation lamp) and images were collected using an iPhone camera.

*SDS-PAGE (Sodium Dodecyl Sulfate–Polyacrylamide Gel Electrophoresis) Measurements.* These measurements were aimed at identifying the strongly adsorbed protein (or hard corona protein). For a typical measurement, the following steps were applied to the QD dispersions after exposure to the media. (1) A 52.8 μL aliquot of 2.13 μM stock QD dispersion was diluted in PBS buffer to a total volume of 500 μL (a final conc. of ∼0.22 μM), which was first incubated with 10% FBS for varying time periods. (2) The dispersion was then added to a sucrose cushion (0.7 M, 500 μL) in an 1.5 mL Eppendorf tube, without mixing, and then centrifuged at 13,000 rpm (i.e., ∼15,000 *g*) for 20 min at 4 °C. The supernatant was discarded and the pellet redispersed in PBS buffer (250 μL). The procedure was then repeated twice. An additional round of centrifugation at 13,000 rpm, 4 °C for 20 min, was applied to the dispersion, the supernatant was discarded, and the pellet (which contain only QDs with the strongly adsorbed protein) was redispersed in 2× Laemmli buffer (with 5% BME), then incubated at 100 °C for 5 min, to allow denaturing and release of the protein from the nanocrystal surfaces. One round of room temperature centrifugation at 13,000 rpm for 15 min was applied to the above mixture in order to precipitate the freed QDs. The resulting supernatant (containing the proteins) was transferred to a fresh tube. The concentration of Laemmli buffer in the sample solution was diluted to 1× using PBS buffer prior to use. 20 μL aliquots of the above solution were loaded on 10% SDS polyacrylamide gel and run using 12 V/cm for 1.5 h; this facilitates the separation of distinct protein based on molecular weights. An EZ-Run Pre-Stained Rec Protein Ladder was used as the molecular weight standards.

## ■ ASSOCIATED CONTENT

### Supporting Information

The Supporting Information is available free of charge on the ACS Publications website at DOI: 10.1021/acs.bioconjchem.9b00549.

Materials information, additional experimental details, synthesis of additional DHLA-modified ligands, UV absorption and PL emission spectra of representative QDs surface ligated with DHLA-appended ligands, standard BSA curves used to quantify the amounts of "hard coronae" on QDs, additional agarose gel and SDS–polyacrylamide gel electrophoresis images, and densitometry analysis (PDF)

## ■ AUTHOR INFORMATION


### Corresponding Author

*E-mail: hmattoussi@fsu.edu.

### ORCID

Wentao Wang: 0000-0003-2273-4171

Hedi Mattoussi: 0000-0002-6511-9323

### Present Addresses

[†]The Food and Drug Administration, National Center for Toxicological Research, 3900 NCTR Road, Jefferson, AR 72079, USA

[‡]Xen Biofluidx, Inc., 11494 Sorrento Valley Rd., San Diego, CA 92121, USA


### Notes

The authors declare no competing financial interest.

## ■ ACKNOWLEDGMENTS

We thank Florida State University, the National Science Foundation (NSF-CHE, Grant 1508501), AFOSR (Grant #FA9550-18-1-0144), and Asahi-Kasei for financial support. We also thank Isabel Askenasy, Joe Pennington, and Christian Escobar for the fruitful discussions.

## ■ REFERENCES


(1) Murray, C. B., Norris, D. J., and Bawendi, M. G. (1993) Synthesis and Characterization of Nearly Monodisperse Cde (E = S, Se, Te) Semiconductor Nanocrystallites. *J. Am. Chem. Soc. 115*, 8706–8715.

(2) Peng, Z. A., and Peng, X. (2001) Formation of High-Quality CdTe, CdSe, and CdS Nanocrystals Using CdO as Precursor. *J. Am. Chem. Soc. 123*, 183–184.

(3) Talapin, D. V., Lee, J. S., Kovalenko, M. V., and Shevchenko, E. V. (2010) Prospects of Colloidal Nanocrystals for Electronic and Optoelectronic Applications. *Chem. Rev. 110*, 389–458.

(4) Kovalenko, M. V., Manna, L., Cabot, A., Hens, Z., Talapin, D. V., Kagan, C. R., Klimov, V. I., Rogach, A. L., Reiss, P., Milliron, D. J., et al. (2015) Prospects of Nanoscience with Nanocrystals. *ACS Nano 9*, 1012–1057.

(5) Kagan, C. R., Lifshitz, E., Sargent, E. H., and Talapin, D. V. (2016) Building devices from colloidal quantum dots. *Science 353*, 6302.

(6) Larson, D. R., Zipfel, W. R., Williams, R. M., Clark, S. W., Bruchez, M. P., Wise, F. W., and Webb, W. W. (2003) Water-soluble quantum dots for multiphoton fluorescence imaging in vivo. *Science 300*, 1434–1436.

(7) Clapp, A. R., Pons, T., Medintz, I. L., Delehanty, J. B., Melinger, J. S., Tiefenbrunn, T., Dawson, P. E., Fisher, B. R., O'Rourke, B., and




DOI: 10.1021/acs.bioconjchem.9b00549
*Bioconjugate Chem.* 2019, 30, 2469–2480

Mattoussi, H. (2007) Two-photon excitation of quantum-dot-based fluorescence resonance energy transfer and its applications. *Adv. Mater. 19*, 1921−1926.
(8) Dabbousi, B. O., Rodriguez-Viejo, J., Mikulec, F. V., Heine, J. R., Mattoussi, H., Ober, R., Jensen, K. F., and Bawendi, M. G. (1997) (CdSe)ZnS Core-Shell Quantum Dots: Synthesis and Characterization of a Size Series of Highly Luminescent Nanocrystallites. *J. Phys. Chem. B 101*, 9463−9475.
(9) Hines, M. A., and Guyot-Sionnest, P. (1996) Synthesis and Characterization of Strongly Luminescing ZnS-Capped CdSe Nanocrystals. *J. Phys. Chem. 100*, 468−471.
(10) Reiss, P., Bleuse, J., and Pron, A. (2002) Highly Luminescent CdSe/ZnSe Core/Shell Nanocrystals of Low Size Dispersion. *Nano Lett. 2*, 781−784.
(11) Jaiswal, J. K., Mattoussi, H., Mauro, J. M., and Simon, S. M. (2003) Long-term multiple color imaging of live cells using quantum dot bioconjugates. *Nat. Biotechnol. 21*, 47−51.
(12) Chan, W. C. W., and Nie, S. (1998) Quantum Dot Bioconjugates for Ultrasensitive Nonisotopic Detection. *Science 281*, 2016−2018.
(13) Bruchez, M., Moronne, M., Gin, P., Weiss, S., and Alivisatos, A. P. (1998) Semiconductor Nanocrystals as Fluorescent Biological Labels. *Science 281*, 2013−2016.
(14) Wu, X., Liu, H., Liu, J., Haley, K. N., Treadway, J. A., Larson, J. P., Ge, N., Peale, F., and Bruchez, M. P. (2003) Immunofluorescent labeling of cancer marker Her2 and other cellular targets with semiconductor quantum dots. *Nat. Biotechnol. 21*, 41−46.
(15) Gao, X., Cui, Y., Levenson, R. M., Chung, L. W. K., and Nie, S. (2004) In vivo cancer targeting and imaging with semiconductor quantum dots. *Nat. Biotechnol. 22*, 969−976.
(16) Medintz, I. L., Uyeda, H. T., Goldman, E. R., and Mattoussi, H. (2005) Quantum dot bioconjugates for imaging, labelling and sensing. *Nat. Mater. 4*, 435−446.
(17) Michalet, X., Pinaud, F. F., Bentolila, L. A., Tsay, J. M., Doose, S., Li, J. J., Sundaresan, G., Wu, A. M., Gambhir, S. S., and Weiss, S. (2005) Quantum Dots for Live Cells, in Vivo Imaging, and Diagnostics. *Science 307*, 538−544.
(18) Resch-Genger, U., Grabolle, M., Cavaliere-Jaricot, S., Nitschke, R., and Nann, T. (2008) Quantum dots versus organic dyes as fluorescent labels. *Nat. Methods 5*, 763−775.
(19) Gill, R., Zayats, M., and Willner, I. (2008) Semiconductor Quantum Dots for Bioanalysis. *Angew. Chem., Int. Ed. 47*, 7602−7625.
(20) Mattoussi, H., Palui, G., and Na, H. B. (2012) Luminescent quantum dots as platforms for probing in vitro and in vivo biological processes. *Adv. Drug Delivery Rev. 64*, 138−166.
(21) Zrazhevskiy, P., Sena, M., and Gao, X. (2010) Designing multifunctional quantum dots for bioimaging, detection, and drug delivery. *Chem. Soc. Rev. 39*, 4326−4354.
(22) Hamad-Schifferli, K. (2013) How can we exploit the protein corona? *Nanomedicine 8*, 1−3.
(23) Lynch, I., and Dawson, K. A. (2008) Protein-nanoparticle interactions. *Nano Today 3*, 40−47.
(24) Nel, A. E., Madler, L., Velegol, D., Xia, T., Hoek, E. M. V., Somasundaran, P., Klaessig, F., Castranova, V., and Thompson, M. (2009) Understanding biophysicochemical interactions at the nano-bio interface. *Nat. Mater. 8*, 543−557.
(25) Pino, P. d., Pelaz, B., Zhang, Q., Maffre, P., Nienhaus, G. U., and Parak, W. J. (2014) Protein corona formation around nanoparticles - from the past to the future. *Mater. Horiz. 1*, 301−313.
(26) Vilaseca, P., Dawson, K. A., and Franzese, G. (2013) Understanding and modulating the competitive surface-adsorption of proteins through coarse-grained molecular dynamics simulations. *Soft Matter 9*, 6978−6985.
(27) Lynch, I., Cedervall, T., Lundqvist, M., Cabaleiro-Lago, C., Linse, S., and Dawson, K. A. (2007) The nanoparticle-protein complex as a biological entity; a complex fluids and surface science challenge for the 21st century. *Adv. Colloid Interface Sci. 134*, 167−174.
(28) Docter, D., Westmeier, D., Markiewicz, M., Stolte, S., Knauer, S. K., and Stauber, R. H. (2015) The nanoparticle biomolecule corona: lessons learned - challenge accepted? *Chem. Soc. Rev. 44*, 6094−6121.
(29) Rocker, C., Potzl, M., Zhang, F., Parak, W. J., and Nienhaus, G. U. (2009) A quantitative fluorescence study of protein monolayer formation on colloidal nanoparticles. *Nat. Nanotechnol. 4*, 577−580.
(30) Salvati, A., Pitek, A. S., Monopoli, M. P., Prapainop, K., Bombelli, F. B., Hristov, D. R., Kelly, P. M., Aberg, C., Mahon, E., and Dawson, K. A. (2013) Transferrin-functionalized nanoparticles lose their targeting capabilities when a biomolecule corona adsorbs on the surface. *Nat. Nanotechnol. 8*, 137−143.
(31) Shannahan, J. H., Lai, X., Ke, P. C., Podila, R., Brown, J. M., and Witzmann, F. A. (2013) Silver Nanoparticle Protein Corona Composition in Cell Culture Media. *PLoS One 8*, No. e74001.
(32) Lundqvist, M., Stigler, J., Elia, G., Lynch, I., Cedervall, T., and Dawson, K. A. (2008) Nanoparticle size and surface properties determine the protein corona with possible implications for biological impacts. *Proc. Natl. Acad. Sci. U. S. A. 105*, 14265−14270.
(33) Mahmoudi, M., Abdelmonem, A. M., Behzadi, S., Clement, J. H., Dutz, S., Ejtehadi, M. R., Hartmann, R., Kantner, K., Linne, U., Maffre, P., et al. (2013) Temperature: The "Ignored" Factor at the NanoBio Interface. *ACS Nano 7*, 6555−6562.
(34) Tenzer, S., Docter, D., Rosfa, S., Wlodarski, A., Kuharev, J., Rekik, A., Knauer, S. K., Bantz, C., Nawroth, T., Bier, C., et al. (2011) Nanoparticle Size Is a Critical Physicochemical Determinant of the Human Blood Plasma Corona: A Comprehensive Quantitative Proteomic Analysis. *ACS Nano 5*, 7155−7167.
(35) Piella, J., Bastús, N. G., and Puntes, V. (2017) Size-Dependent Protein-Nanoparticle Interactions in Citrate-Stabilized Gold Nanoparticles: The Emergence of the Protein Corona. *Bioconjugate Chem. 28*, 88−97.
(36) Barrán-Berdón, A. L., Pozzi, D., Caracciolo, G., Capriotti, A. L., Caruso, G., Cavaliere, C., Riccioli, A., Palchetti, S., and Laganà, A. (2013) Time Evolution of Nanoparticle-Protein Corona in Human Plasma: Relevance for Targeted Drug Delivery. *Langmuir 29*, 6485−6494.
(37) Casals, E., Pfaller, T., Duschl, A., Oostingh, G. J., and Puntes, V. (2010) Time Evolution of the Nanoparticle Protein Corona. *ACS Nano 4*, 3623−3632.
(38) Tenzer, S., Docter, D., Kuharev, J., Musyanovych, A., Fetz, V., Hecht, R., Schlenk, F., Fischer, D., Kiouptsi, K., Reinhardt, C., et al. (2013) Rapid formation of plasma protein corona critically affects nanoparticle pathophysiology. *Nat. Nanotechnol. 8*, 772−781.
(39) Caracciolo, G., Pozzi, D., Capriotti, A. L., Cavaliere, C., Foglia, P., Amenitsch, H., and Laganà, A. (2011) Evolution of the Protein Corona of Lipid Gene Vectors as a Function of Plasma Concentration. *Langmuir 27*, 15048−15053.
(40) Monopoli, M. P., Walczyk, D., Campbell, A., Elia, G., Lynch, I., Baldelli Bombelli, F., and Dawson, K. A. (2011) Physical-Chemical Aspects of Protein Corona: Relevance to in Vitro and in Vivo Biological Impacts of Nanoparticles. *J. Am. Chem. Soc. 133*, 2525−2534.
(41) Ehrenberg, M. S., Friedman, A. E., Finkelstein, J. N., Oberdorster, G., and McGrath, J. L. (2009) The influence of protein adsorption on nanoparticle association with cultured endothelial cells. *Biomaterials 30*, 603−610.
(42) Walkey, C. D., Olsen, J. B., Guo, H., Emili, A., and Chan, W. C. W. (2012) Nanoparticle Size and Surface Chemistry Determine Serum Protein Adsorption and Macrophage Uptake. *J. Am. Chem. Soc. 134*, 2139−2147.
(43) Walczyk, D., Bombelli, F. B., Monopoli, M. P., Lynch, I., and Dawson, K. A. (2010) What the Cell "Sees" in Bionanoscience. *J. Am. Chem. Soc. 132*, 5761−5768.
(44) Hadjidemetriou, M., Al-Ahmady, Z., and Kostarelos, K. (2016) Time-evolution of in vivo protein corona onto blood-circulating PEGylated liposomal doxorubicin (DOXIL) nanoparticles. *Nanoscale 8*, 6948−6957.


DOI: 10.1021/acs.bioconjchem.9b00549
*Bioconjugate Chem.* 2019, 30, 2469−2480

(45) Pelaz, B., del Pino, P., Maffre, P., Hartmann, R., Gallego, M., Rivera-Fernández, S., de la Fuente, J. M., Nienhaus, G. U., and Parak, W. J. (2015) Surface Functionalization of Nanoparticles with Polyethylene Glycol: Effects on Protein Adsorption and Cellular Uptake. *ACS Nano 9*, 6996−7008.
(46) Wattendorf, U., and Merkle, H. P. (2008) PEGylation as a tool for the biomedical engineering of surface modified microparticles. *J. Pharm. Sci. 97*, 4655−4669.
(47) García, I., Sánchez-Iglesias, A., Henriksen-Lacey, M., Grzelczak, M., Penadés, S., and Liz-Marzán, L. M. (2015) Glycans as Biofunctional Ligands for Gold Nanorods: Stability and Targeting in Protein-Rich Media. *J. Am. Chem. Soc. 137*, 3686−3692.
(48) Pozzi, D., Colapicchioni, V., Caracciolo, G., Piovesana, S., Capriotti, A. L., Palchetti, S., De Grossi, S., Riccioli, A., Amenitsch, H., and Lagana, A. (2014) Effect of polyethyleneglycol (PEG) chain length on the bio-nano-interactions between PEGylated lipid nanoparticles and biological fluids: from nanostructure to uptake in cancer cells. *Nanoscale 6*, 2782−2792.
(49) Moyano, D. F., Saha, K., Prakash, G., Yan, B., Kong, H., Yazdani, M., and Rotello, V. M. (2014) Fabrication of Corona-Free Nanoparticles with Tunable Hydrophobicity. *ACS Nano 8*, 6748−6755.
(50) Wei, H., Insin, N., Lee, J., Han, H.-S., Cordero, J. M., Liu, W., and Bawendi, M. G. (2012) Compact Zwitterion-Coated Iron Oxide Nanoparticles for Biological Applications. *Nano Lett. 12*, 22−25.
(51) García, K. P., Zarschler, K., Barbaro, L., Barreto, J. A., O'Malley, W., Spiccia, L., Stephan, H., and Graham, B. (2014) Zwitterionic-Coated "Stealth" Nanoparticles for Biomedical Applications: Recent Advances in Countering Biomolecular Corona Formation and Uptake by the Mononuclear Phagocyte System. *Small 10*, 2516−2529.
(52) Guerrini, L., Alvarez-Puebla, R. A., and Pazos-Perez, N. (2018) Surface Modifications of Nanoparticles for Stability in Biological Fluids. *Materials 11*, 1154.
(53) Debayle, M., Balloul, E., Dembele, F., Xu, X., Hanafi, M., Ribot, F., Monzel, C., Coppey, M., Fragola, A., Dahan, M., et al. (2019) Zwitterionic polymer ligands: an ideal surface coating to totally suppress protein-nanoparticle corona formation? *Biomaterials 219*, 119357.
(54) Zheng, X., Baker, H., Hancock, W. S., Fawaz, F., McCaman, M., and Pungor, E. (2006) Proteomic Analysis for the Assessment of Different Lots of Fetal Bovine Serum as a Raw Material for Cell Culture. Part IV. Application of Proteomics to the Manufacture of Biological Drugs. *Biotechnol. Progr. Biotechnol. Progr. Biotechnol. Progr. 22*, 1294−1300.
(55) Sperling, R. A., and Parak, W. J. (2010) Surface modification, functionalization and bioconjugation of colloidal inorganic nanoparticles. *Philos. Trans. R. Soc., A 368*, 1333−1383.
(56) Palui, G., Aldeek, F., Wang, W. T., and Mattoussi, H. (2015) Strategies for interfacing inorganic nanocrystals with biological systems based on polymer-coating. *Chem. Soc. Rev. 44*, 193−227.
(57) Zhang, F., Lees, E., Amin, F., Rivera Gil, P., Yang, F., Mulvaney, P., and Parak, W. J. (2011) Polymer-Coated Nanoparticles: A Universal Tool for Biolabelling Experiments. *Small 7*, 3113−3127.
(58) Sapsford, K. E., Algar, W. R., Berti, L., Gemmill, K. B., Casey, B. J., Oh, E., Stewart, M. H., and Medintz, I. L. (2013) Functionalizing Nanoparticles with Biological Molecules: Developing Chemistries that Facilitate Nanotechnology. *Chem. Rev. 113*, 1904−2074.
(59) Nam, J., Won, N., Bang, J., Jin, H., Park, J., Jung, S., Jung, S., Park, Y., and Kim, S. (2013) Surface engineering of inorganic nanoparticles for imaging and therapy. *Adv. Drug Delivery Rev. 65*, 622−648.
(60) Chou, L. Y. T., Ming, K., and Chan, W. C. W. (2011) Strategies for the intracellular delivery of nanoparticles. *Chem. Soc. Rev. 40*, 233−245.
(61) Mattoussi, H., Mauro, J. M., Goldman, E. R., Anderson, G. P., Sundar, V. C., Mikulec, F. V., and Bawendi, M. G. (2000) Self-assembly of CdSe-ZnS quantum dot bioconjugates using an engineered recombinant protein. *J. Am. Chem. Soc. 122*, 12142−12150.
(62) Mei, B. C., Susumu, K., Medintz, I. L., Delehanty, J. B., Mountziaris, T. J., and Mattoussi, H. (2008) Modular poly(ethylene glycol) ligands for biocompatible semiconductor and gold nanocrystals with extended pH and ionic stability. *J. Mater. Chem. 18*, 4949−4958.
(63) Clapp, A. R., Goldman, E. R., and Mattoussi, H. (2006) Capping of CdSe-ZnS quantum dots with DHLA and subsequent conjugation with proteins. *Nat. Protoc. 1*, 1258−1266.
(64) Pons, T., Uyeda, H. T., Medintz, I. L., and Mattoussi, H. (2006) Hydrodynamic Dimensions, Electrophoretic Mobility, and Stability of Hydrophilic Quantum Dots. *J. Phys. Chem. B 110*, 20308−20316.
(65) Uyeda, H. T., Medintz, I. L., Jaiswal, J. K., Simon, S. M., and Mattoussi, H. (2005) Synthesis of Compact Multidentate Ligands to Prepare Stable Hydrophilic Quantum Dot Fluorophores. *J. Am. Chem. Soc. 127*, 3870−3878.
(66) Liu, W., Choi, H. S., Zimmer, J. P., Tanaka, E., Frangioni, J. V., and Bawendi, M. (2007) Compact Cysteine-Coated CdSe(ZnCdS) Quantum Dots for in Vivo Applications. *J. Am. Chem. Soc. 129*, 14530−14531.
(67) Medintz, I. L., Clapp, A. R., Mattoussi, H., Goldman, E. R., Fisher, B., and Mauro, J. M. (2003) Self-assembled nanoscale biosensors based on quantum dot FRET donors. *Nat. Mater. 2*, 630−638.
(68) Susumu, K., Uyeda, H. T., Medintz, I. L., Pons, T., Delehanty, J. B., and Mattoussi, H. (2007) Enhancing the stability and biological functionalities of quantum dots via compact multifunctional ligands. *J. Am. Chem. Soc. 129*, 13987−13996.
(69) Medintz, I. L., and Mattoussi, H. (2009) Quantum dot-based resonance energy transfer and its growing application in biology. *Phys. Chem. Chem. Phys. 11*, 17−45.
(70) Goldman, E. R., Clapp, A. R., Anderson, G. P., Uyeda, H. T., Mauro, J. M., Medintz, I. L., and Mattoussi, H. (2004) Multiplexed toxin analysis using four colors of quantum dot fluororeagents. *Anal. Chem. 76*, 684−688.
(71) Hill, A. V. (1910) The possible effects of the aggregation of the molecules of huemoglobin on its dissociation curves. *Proc. Phys. Society: J. Physiol. 40*, i−vii.
(72) Gesztelyi, R., Zsuga, J., Kemeny-Beke, A., Varga, B., Juhasz, B., and Tosaki, A. (2012) The Hill equation and the origin of quantitative pharmacology. *Arch. Hist. Exact Sci. 66*, 427−438.
(73) Kapur, A., Aldeek, F., Ji, X., Safi, M., Wang, W., Del Cid, A., Steinbock, O., and Mattoussi, H. (2017) Self-Assembled Gold Nanoparticle-Fluorescent Protein Conjugates as Platforms for Sensing Thiolate Compounds via Modulation of Energy Transfer Quenching. *Bioconjugate Chem. 28*, 678−687.
(74) Sapsford, K. E., Pons, T., Medintz, I. L., Higashiya, S., Brunel, F. M., Dawson, P. E., and Mattoussi, H. (2007) Kinetics of metal-affinity driven self-assembly between proteins or peptides and CdSe-ZnS quantum dots. *J. Phys. Chem. C 111*, 11528−11538.
(75) Treuel, L., Brandholt, S., Maffre, P., Wiegele, S., Shang, L., and Nienhaus, G. U. (2014) Impact of Protein Modification on the Protein Corona on Nanoparticles and Nanoparticle-Cell Interactions. *ACS Nano 8*, 503−513.
(76) Wang, H., Shang, L., Maffre, P., Hohmann, S., Kirschhöfer, F., Brenner-Weiß, G., and Nienhaus, G. U. (2016) The Nature of a Hard Protein Corona Forming on Quantum Dots Exposed to Human Blood Serum. *Small 12*, 5836−5844.
(77) Goldman, E. R., Medintz, I. L., Hayhurst, A., Anderson, G. P., Mauro, J. M., Iverson, B. L., Georgiou, G., and Mattoussi, H. (2005) Self-assembled luminescent CdSe-ZnS quantum dot bioconjugates prepared using engineered poly-histidine terminated proteins. *Anal. Chim. Acta 534*, 63−67.
(78) Wang, W., Ji, X., Kapur, A., Zhang, C., and Mattoussi, H. (2015) A Multifunctional Polymer Combining the Imidazole and Zwitterion Motifs as a Biocompatible Compact Coating for Quantum Dots. *J. Am. Chem. Soc. 137*, 14158−14172.
(79) Pearson, R. G. (1963) Hard and Soft Acids and Bases. *J. Am. Chem. Soc. 85*, 3533−3539.


DOI: 10.1021/acs.bioconjchem.9b00549
*Bioconjugate Chem.* 2019, 30, 2469−2480

(80) Ashraf, S., Park, J., Bichelberger, M. A., Kantner, K., Hartmann, R., Maffre, P., Said, A. H., Feliu, N., Lee, J., Lee, D., et al. (2016) Zwitterionic surface coating of quantum dots reduces protein adsorption and cellular uptake. *Nanoscale 8*, 17794−17800.
(81) Schlenoff, J. B. (2014) Zwitteration: Coating Surfaces with Zwitterionic Functionality to Reduce Nonspecific Adsorption. *Langmuir 30*, 9625−9636.
(82) Welsher, K., McManus, S. A., Hsia, C.-H., Yin, S., and Yang, H. (2015) Discovery of Protein- and DNA-Imperceptible Nanoparticle Hard Coating Using Gel-Based Reaction Tuning. *J. Am. Chem. Soc. 137*, 580−583.
(83) Hu, Y., Xie, J., Tong, Y. W., and Wang, C.-H. (2007) Effect of PEG conformation and particle size on the cellular uptake efficiency of nanoparticles with the HepG2 cells. *J. Controlled Release 118*, 7−17.
(84) Susumu, K., Mei, B. C., and Mattoussi, H. (2009) Multifunctional ligands based on dihydrolipoic acid and polyethylene glycol to promote biocompatibility of quantum dots. *Nat. Protoc. 4*, 424−436.
(85) Lynch, I., and Dawson, K. A. (2008) Protein-nanoparticle interactions. *Nano Today 3*, 40−47.
(86) Vroman, L., Adams, A., Fischer, G., and Munoz, P. (1980) Interaction of high molecular weight kininogen, factor XII, and fibrinogen in plasma at interfaces. *Blood 55*, 156−159.
(87) Liu, W., Howarth, M., Greytak, A. B., Zheng, Y., Nocera, D. G., Ting, A. Y., and Bawendi, M. G. (2008) Compact biocompatible quantum dots functionalized for cellular imaging. *J. Am. Chem. Soc. 130*, 1274−1284.
(88) Docter, D., Distler, U., Storck, W., Kuharev, J., Wünsch, D., Hahlbrock, A., Knauer, S. K., Tenzer, S., and Stauber, R. H. (2014) Quantitative profiling of the protein coronas that form around nanoparticles. *Nat. Protoc. 9*, 2030.
(89) Mei, B. C., Susumu, K., Medintz, I. L., and Mattoussi, H. (2009) Polyethylene glycol-based bidentate ligands to enhance quantum dot and gold nanoparticle stability in biological media. *Nat. Protoc. 4*, 412−423.
(90) Zhan, N., Palui, G., and Mattoussi, H. (2015) Preparation of compact biocompatible quantum dots using multicoordinating molecular-scale ligands based on a zwitterionic hydrophilic motif and lipoic acid anchors. *Nat. Protoc. 10*, 859−874.
(91) Palui, G., Avellini, T., Zhan, N., Pan, F., Gray, D., Alabugin, I., and Mattoussi, H. (2012) Photoinduced Phase Transfer of Luminescent Quantum Dots to Polar and Aqueous Media. *J. Am. Chem. Soc. 134*, 16370−16378.


DOI: 10.1021/acs.bioconjchem.9b00549
*Bioconjugate Chem.* 2019, 30, 2469−2480